RIGOROUS ANALYSIS OF TM WAVE SCATTERING BY A LARGE CIRCUMFERENTIAL GAP ON A DIELECTRIC-FILLED CIRCULAR WAVEGUIDE

Hülya Öztürk[1], Gökhan Cinar[2], Özge Yanaz Cinar[3]

TM wave scattering by a large circumferential gap on a circular waveguide filled with a dielectric material is investigated rigorously by applying direct Fourier transform and reducing the problem into the solution of a modified Wiener-Hopf equation of the first type. Classical Wiener-Hopf procedure is applied and the Wiener-Hopf equation is solved via a set of Fredholm integral equations of the second type. At the end of the analysis, the effects of waveguide radius, relative permittivity, frequency and the gap width on the scattered fields are illustrated graphically.

Keywords: Fourier transform, Wiener-Hopf, Scattering, Circular waveguide
MSC2010: 78AK5, 47A68, 42B10.

1. Introduction

The problem of scattering of electromagnetic waves along waveguides with gaps on their walls has become more interesting for scientists and engineers. It has been extensively studied in the literature, such as microwave bandpass filters, measurement devices, and waveguide radiators. Due to the need of more accurate modeling of related engineering applications of practical importance, analytical methods has recently increased [3,12,13]. In 1954, Sheingold and Storer analyzed a circular waveguide with a gap on its wall in the case of TE wave incidence by using variational principle [14]. They found good agreement with experiments for narrow gaps (small gap width to the wavelength). Later, in 1968, Morita and Nakanishi investigated the same problem by means of fictitious equivalent magnetic current for the gap [7]. They compared the results with the analysis obtained by Bethe's method and two results agreed well for narrow gaps. Besides, Lawrie [5] has analyzed the acoustic scattering problem by a finite gap in an infinite, rigid, circular duct. For circular waveguides, the case where the gap on the wall of a waveguide is large compared to the wavelength is studied by Elmoazzen and Shafai for TM wave incidence and air-filled waveguides, where they applied direct Fourier transform and reduced the problem into solving a modified Wiener–Hopf technique of the first kind [4]. The resulting Fredholm integral equation of the second type is solved for large gap width compared to the wavelength. The same problem is then analyzed by Park and Eom in 2003 for thick walls and field expressions are determined by applying a new method based on Fourier transform and series representation techniques [10]. More recently, the authors of this paper have analyzed TEM wave scattering by a hollow and dielectric-filled coaxial waveguides having a large circumferential gap on its outer wall [8,9]. In this paper, TM wave scattering by a large circumferential gap on the

[1]Dr., Department of Mathematics, Gebze Technical University, Kocaeli, Turkey, e-mail: h.ozturk@gtu.edu.tr
[2]Prof., Electrical and Electronics Engineering Department, Eskisehir Osmangazi University, Eskisehir, Turkey
[3]Assoc. Prof. Dr., Electrical and Electronics Engineering Department, Eskisehir Osmangazi University, Eskisehir, Turkey

wall of a dielectric-filled circular waveguide is analyzed rigorously by applying direct Fourier transform which yields a modified Wiener–Hopf equation of the first type as [1,2,11,15]. This modified Wiener–Hopf equation is reduced to a Fredholm integral equation of the second type which is solved in a similar fashion as in [11]. Finally, the diffraction coefficients related to the reflected, transmitted, and radiated fields are determined explicitly. At the end of the analysis, numerical results illustrating the effects of the waveguide radius, the relative permittivity of the dielectric material inside the waveguide and the gap width on the radiated field are presented. A time dependence $\mathrm{e}^{-\mathrm{i}\omega t}$ with ω being the angular frequency is assumed and suppressed throughout the paper.

2. **Formulation of the problem**

Consider a dielectric-filled circular waveguide whose wall is located at $S = \{\rho = a, (-\infty < z < 0) \cup (l < z < \infty)\}$ (see Figure 1) and assume an incident TM_{0n} wave propagating in the positive $z-$direction, with an electric hertz vector given by

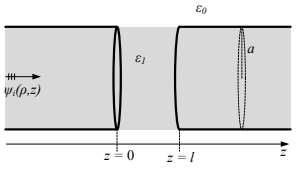

Fig. 1. The geometry of the problem.

$$\mathbf{\Pi}_i(\rho, z) = \psi_i(\rho, z)\,\mathbf{a}_z \tag{1}$$

where the potential function $\psi_i(\rho, z)$ stands for

$$\psi_i(\rho, z) = \mathrm{J}_0(K_n\rho)\,\mathrm{e}^{\mathrm{i}\alpha_n z}. \tag{2}$$

Here K_n's satisfy

$$\mathrm{J}_0(K_n a) = 0, \quad n = 1, 2, 3, ... \tag{3}$$

with

$$\alpha_n = \sqrt{k_1^2 - \left(\frac{K_n}{a}\right)^2}, \quad n = 1, 2, 3, ... \tag{4}$$

and $\mathrm{J}_n(z)$ being the usual Bessel function of the first type. Here, k_1 is the propagation constant inside the waveguide, which is assumed to have a small imaginary part corresponding to slightly lossy medium. The lossless case can then be obtained by letting $\Im m(k_1) \to 0$ at the end of the analysis. In virtue of the axial symmetry of the problem, all the field components may be expressed in terms of $\psi(\rho, z)$ as

$$E_\rho = \frac{\mathrm{i}}{\omega\varepsilon}\frac{\partial^2\psi(\rho, z)}{\partial\rho\partial z}, \quad E_z = \frac{\mathrm{i}}{\omega\varepsilon}\left(\frac{\partial^2}{\partial z^2} + k^2\right)\psi(\rho, z) \quad \text{and} \quad H_\phi = -\frac{\partial\psi(\rho, z)}{\partial\rho}.$$

Hence, the field components of the incident wave become

$$E_\rho^i = \frac{\alpha_n K_n}{\omega\varepsilon_1}\mathrm{J}_1(K_n\rho)\,\mathrm{e}^{\mathrm{i}\alpha_n z}, \quad E_z^i = \frac{\mathrm{i}K_n^2}{\omega\varepsilon_1}\mathrm{J}_0(K_n\rho)\,\mathrm{e}^{\mathrm{i}\alpha_n z} \quad \text{and} \quad H_\phi^i = K_n\mathrm{J}_1(K_n\rho)\,\mathrm{e}^{\mathrm{i}\alpha_n z}.$$

For the sake of analytical convenience, the total field can be written as

$$\psi_T(\rho, z) = \begin{cases} \psi_i(\rho, z) + \psi_1(\rho, z) & , \quad \rho < a \\ \psi_2(\rho, z) & , \quad \rho > a \end{cases} \tag{5}$$

where $\psi_1(\rho,z)$ and $\psi_2(\rho,z)$ are the scattered fields which satisfy the Helmholtz equations

$$\left[\frac{\partial^2}{\partial\rho^2}+\frac{1}{\rho}\frac{\partial}{\partial\rho}+\frac{\partial}{\partial z^2}+k_1^2\right]\psi_1(\rho,z)=0,\quad \rho<a \tag{6}$$

$$\left[\frac{\partial^2}{\partial\rho^2}+\frac{1}{\rho}\frac{\partial}{\partial\rho}+\frac{\partial}{\partial z^2}+k_0^2\right]\psi_2(\rho,z)=0,\quad \rho>a \tag{7}$$

with the boundary conditions

$$\psi_1(a,z)=0\ ,\quad z\in(-\infty,0)\cup(l,\infty)\,, \tag{8}$$

$$\psi_2(a,z)=0\ ,\quad z\in(-\infty,0)\cup(l,\infty) \tag{9}$$

and the continuity relations

$$\frac{1}{\varepsilon_1}\left(\frac{\partial^2}{\partial z^2}+k_1^2\right)\psi_1(a,z)=\frac{1}{\varepsilon_0}\left(\frac{\partial^2}{\partial z^2}+k_0^2\right)\psi_2(a,z)\ ,\quad z\in(0,l) \tag{10}$$

and

$$K_n\mathrm{J}_1(K_na)\,\mathrm{e}^{\mathrm{i}\alpha_n z}-\frac{\partial\psi_1(a,z)}{\partial\rho}=-\frac{\partial\psi_2(a,z)}{\partial\rho}\ ,\quad z\in(0,l)\,. \tag{11}$$

Additionally, to ensure the uniqueness of the solution, one has to take into account the radiation and edge conditions as described in [6]. In (7) and (10), k_0 stands for the propagation constant outside the waveguide, which is also assumed to have a small imaginary part.

The Fourier transform of the Helmholtz equation satisfied by $\psi_1(\rho,z)$ with respect to z, in the range of $z\in(-\infty,\infty)$ gives

$$\left[\frac{\partial^2}{\partial\rho^2}+\frac{1}{\rho}\frac{\partial}{\partial\rho}+K_1^2(\alpha)\right]F(\rho,\alpha)=0. \tag{12}$$

Here $K_1(\alpha)=\sqrt{k_1^2-\alpha^2}$ is the square-root function defined in the complex $\alpha-$plane ,cut along $\alpha=k_1$ to $\alpha=k_1+\mathrm{i}\infty$ and $\alpha=-k_1$ to $\alpha=-k_1-\mathrm{i}\infty$, such that $K_1(0)=k_1$ as seen in Figure 2, and the Fourier transform is

$$F(\rho,\alpha)=F_-(\rho,\alpha)+F_1(\rho,\alpha)+\mathrm{e}^{\mathrm{i}\alpha l}F_+(\rho,\alpha) \tag{13}$$

with

$$F_-(\rho,\alpha)=\int_{-\infty}^{0}\psi_1(\rho,z)\,\mathrm{e}^{\mathrm{i}\alpha z}dz, \tag{14}$$

$$F_1(\rho,\alpha)=\int_{0}^{l}\psi_1(\rho,z)\,\mathrm{e}^{\mathrm{i}\alpha z}dz \tag{15}$$

$$F_+(\rho,\alpha)=\int_{l}^{\infty}\psi_1(\rho,z)\,\mathrm{e}^{\mathrm{i}\alpha(z-l)}dz. \tag{16}$$

Notice that $F_+(\rho,\alpha)$ and $F_-(\rho,\alpha)$ are unknown functions which are regular in the half-

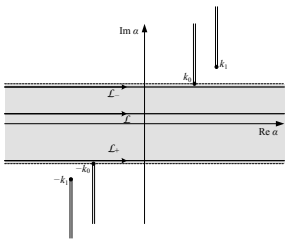

Fig. 2. Complex $\alpha-$plane.

planes $\Im m(\alpha) > \Im m(-k_1)$ and $\Im m(\alpha) < \Im m(k_1)$, respectively, while $F_1(\rho,\alpha)$ is an entire function of α. The general solution of (12) is

$$F(\rho,\alpha) = A(\alpha)\,\mathrm{J}_0(K_1\rho), \tag{17}$$

where $A(\alpha)$ is the unknown spectral coefficient to be found. Applying the Fourier transform of the boundary conditions (8) yields $A(\alpha) = F_1(a,\alpha)/\mathrm{J}_0(K_1 a)$ to give

$$F(\rho,\alpha) = F_1(a,\alpha)\frac{\mathrm{J}_0(K_1\rho)}{\mathrm{J}_0(K_1 a)}. \tag{18}$$

On the other hand, the Fourier transform of the Helmholtz equation satisfied by $\psi_2(\rho,z)$ with respect to z, in the range of $z \in (-\infty,\infty)$ gives

$$\left[\frac{\partial^2}{\partial\rho^2} + \frac{1}{\rho}\frac{\partial}{\partial\rho} + K_0^2(\alpha)\right] G(\rho,\alpha) = 0 \tag{19}$$

where $K_0(\alpha) = \sqrt{k_0^2 - \alpha^2}$ is the square-root function defined in the complex $\alpha-$plane ,cut along $\alpha = k_0$ to $\alpha = k_0 + \mathrm{i}\infty$ and $\alpha = -k_0$ to $\alpha = -k_0 - \mathrm{i}\infty$, such that $K_0(0) = k_0$ as seen in Figure 2, and the Fourier transform is

$$G(\rho,\alpha) = G_-(\rho,\alpha) + G_1(\rho,\alpha) + \mathrm{e}^{\mathrm{i}\alpha l} G_+(\rho,\alpha) \tag{20}$$

with

$$G_-(\rho,\alpha) = \int_{-\infty}^{0} \psi_2(\rho,z)\,\mathrm{e}^{\mathrm{i}\alpha z} dz, \tag{21}$$

$$G_1(\rho,\alpha) = \int_{0}^{l} \psi_2(\rho,z)\,\mathrm{e}^{\mathrm{i}\alpha z} dz \tag{22}$$

$$G_+(\rho,\alpha) = \int_{l}^{\infty} \psi_2(\rho,z)\,\mathrm{e}^{\mathrm{i}\alpha(z-l)} dz. \tag{23}$$

Here, $G_+(\rho,\alpha)$ and $G_-(\rho,\alpha)$ are unknown functions which are regular in the half-planes $\Im m(\alpha) > \Im m(-k_0)$ and $\Im m(\alpha) < \Im m(k_0)$, respectively, while $G_1(\rho,\alpha)$ is an entire function of α. The general solution of (19) is

$$G(\rho,\alpha) = B(\alpha)\,\mathrm{H}_0^{(1)}(K_0\rho), \tag{24}$$

where $B(\alpha)$ is the unknown spectral coefficient to be found. In (24), $\mathrm{H}_n^{(1)}(z)$ stands for the usual Hankel function of the first type. Applying the Fourier transform of the boundary conditions (9) yields $B(\alpha) = G_1(a,\alpha)/\mathrm{H}_0^{(1)}(K_0 a)$ to give

$$G(\rho,\alpha) = G_1(a,\alpha)\frac{\mathrm{H}_0^{(1)}(K_0\rho)}{\mathrm{H}_0^{(1)}(K_0 a)}. \tag{25}$$

Similarly, applying Fourier transform to the continuity relations (10) and (11), one can obtain

$$G_1(a,\alpha) = \frac{\varepsilon_0}{\varepsilon_1}\frac{K_1^2(\alpha)}{K_0^2(\alpha)} F_1(a,\alpha) \tag{26}$$

and

$$G_1'(a,\alpha) = K_n \mathrm{J}_1(K_n a)\frac{\left[1 - \mathrm{e}^{\mathrm{i}(\alpha_n+\alpha)l}\right]}{\mathrm{i}(\alpha_n+\alpha)} + F_1'(a,\alpha), \tag{27}$$

respectively. By taking into account the above equations with (13), (18), (20) and (25), one can get

$$N(\alpha)F_1(a,\alpha) + \mathrm{e}^{\mathrm{i}\alpha l}\left[F_+'(a,\alpha) - G_+'(a,\alpha)\right] + \left[F_-'(a,\alpha) - G_-'(a,\alpha)\right] = \frac{K_n \mathrm{J}_1(K_n a)}{\mathrm{i}(\alpha_n+\alpha)} - \frac{K_n \mathrm{J}_1(K_n a)\,\mathrm{e}^{\mathrm{i}(\alpha_n+\alpha)l}}{\mathrm{i}(\alpha_n+\alpha)} \tag{28}$$

with

$$N(\alpha)=\frac{K_1\mathrm{J}_1(K_1a)}{\mathrm{J}_0(K_1a)}-\frac{\varepsilon_0}{\varepsilon_1}\frac{K_1^2(\alpha)}{K_0^2(\alpha)}\frac{K_0\mathrm{H}_1^{(1)}(K_0a)}{\mathrm{H}_0^{(1)}(K_0a)} \tag{29}$$

Equation (28) is nothing but the modified Wiener-Hopf equation regarding the potential function ψ. By taking into account the relation between ψ and E_z, (28) can be rearranged as

$$\frac{\omega\varepsilon_1}{\mathrm{i}K_0^2(\alpha)}M(\alpha)P_1(a,\alpha)+\mathrm{e}^{\mathrm{i}\alpha l}P_+(\alpha)+P_-(\alpha) = \frac{K_n\mathrm{J}_1(K_na)}{\mathrm{i}(\alpha_n+\alpha)}-\frac{K_n\mathrm{J}_1(K_na)\,\mathrm{e}^{\mathrm{i}(\alpha_n+\alpha)l}}{\mathrm{i}(\alpha_n+\alpha)} \tag{30}$$

with

$$P_1(a,\alpha)=\frac{\mathrm{i}K_1^2(\alpha)}{\omega\varepsilon_1}F_1(a,\alpha), \tag{31}$$

$$P_+(\alpha)=F_+'(a,\alpha)-G_+'(a,\alpha), \tag{32}$$

$$P_-(\alpha)=F_-'(a,\alpha)-G_-'(a,\alpha) \tag{33}$$

and

$$M(\alpha)=\frac{\varepsilon_1K_0^2K_1\mathrm{J}_1(K_1a)\,\mathrm{H}_0^{(1)}(K_0a)-\varepsilon_0K_1^2K_0\mathrm{J}_0(K_1a)\,\mathrm{H}_1^{(1)}(K_0a)}{\varepsilon_1K_1^2\mathrm{J}_0(K_1a)\,\mathrm{H}_0^{(1)}(K_0a)}. \tag{34}$$

Notice that $P_1(\rho,\alpha)$ is the Fourier transform of $E_z(\rho,z)$ in the region $z\in(0,l)$, $\rho<a$. Applying classical Wiener-Hopf procedure to (30) yields

$$\frac{(k_0+\alpha)}{M_+(\alpha)}U(\alpha)=-\frac{1}{2\pi\mathrm{i}}\int_{\mathcal{L}_+}\mathrm{e}^{-\mathrm{i}\tau l}\frac{(k_0+\tau)}{M_+(\tau)}L(\tau)\frac{d\tau}{(\tau-\alpha)} \tag{35}$$

$$\frac{(k_0-\alpha)}{M_-(\alpha)}L(\alpha)=\frac{1}{2\pi\mathrm{i}}\int_{\mathcal{L}_-}\mathrm{e}^{\mathrm{i}\tau l}\frac{(k_0-\tau)}{M_-(\tau)}U(\tau)\frac{d\tau}{(\tau-\alpha)}-\frac{K_n\mathrm{J}_1(K_na)(k_0+\alpha_n)}{\mathrm{i}M_+(\alpha_n)(\alpha_n+\alpha)}. \tag{36}$$

with $U(\alpha)$ and $L(\alpha)$ being defined as

$$U(\alpha)=P_+(\alpha)+\frac{K_n\mathrm{J}_1(K_na)\,e^{i\alpha_nl}}{i(\alpha_n+\alpha)} \tag{37}$$

$$L(\alpha)=P_-(\alpha)-\frac{K_n\mathrm{J}_1(K_na)}{\mathrm{i}(\alpha_n+\alpha)}, \tag{38}$$

respectively. The split functions $M_+(\alpha)$ and $M_-(\alpha)$ can be determined by following the procedure described in [8]. (35) and (36) are Fredholm integral equations of the second type with the paths of integration $\mathcal{L}_+$ and $\mathcal{L}_-$ denoted in Figure 2. Changing the integration variable τ by $-\tau$ in (35) and replacing α by $-\alpha$ in (36) and adding and subtracting the resulting equations reads

$$\frac{(k_0+\alpha)}{M_+(\alpha)}\tilde{U}(\alpha)=\frac{1}{2\pi\mathrm{i}}\int_{\mathcal{L}_-}\mathrm{e}^{\mathrm{i}\tau l}\frac{(k_0-\tau)}{M_-(\tau)}\tilde{U}(\tau)\frac{d\tau}{(\tau+\alpha)}-\frac{K_n\mathrm{J}_1(K_na)(k_0+\alpha_n)}{\mathrm{i}M_+(\alpha_n)(\alpha_n-\alpha)} \tag{39}$$

$$\frac{(k_0+\alpha)}{M_+(\alpha)}\tilde{L}(\alpha)=-\frac{1}{2\pi\mathrm{i}}\int_{\mathcal{L}_-}\mathrm{e}^{\mathrm{i}\tau l}\frac{(k_0-\tau)}{M_-(\tau)}\tilde{L}(\tau)\frac{d\tau}{(\tau+\alpha)}+\frac{K_n\mathrm{J}_1(K_na)(k_0+\alpha_n)}{\mathrm{i}M_+(\alpha_n)(\alpha_n-\alpha)} \tag{40}$$

respectively, where $\tilde{U}(\alpha)$ and $\tilde{L}(\alpha)$ are defined by

$$\tilde{U}(\alpha)=U(\alpha)+L(-\alpha) \tag{41}$$

$$\tilde{L}(\alpha)=U(\alpha)-L(-\alpha). \tag{42}$$

In order to solve the coupled system of integral equations (39) and (40), one can apply the method of successive approximations. When $k_{0,1}l$ is large, $\tilde{U}^{(1)}(\alpha)$ and $\tilde{L}^{(1)}(\alpha)$ are the first order solutions obtained by letting the integrals in (39) and (40) be equal to zero. $\tilde{U}^{(2)}(\alpha)$

and $\tilde{L}^{(2)}(\alpha)$ are the second order solutions which are derived by substituting the unknown functions appearing in the integrands by first order approximations. The same process can be used to obtain the higher-order terms. Hence, one gets

$$\tilde{U}(\alpha)=\tilde{U}^{(1)}(\alpha)+\tilde{U}^{(2)}(\alpha)+\tilde{U}^{(3)}(\alpha)+... \tag{43}$$

$$\tilde{L}(\alpha)=\tilde{L}^{(1)}(\alpha)+\tilde{L}^{(2)}(\alpha)+\tilde{L}^{(3)}(\alpha)+... \tag{44}$$

where the first-order solutions are determined to be

$$\tilde{U}^{(1)}(\alpha)=-\frac{K_n\mathrm{J}_1(K_na)(k_0+\alpha_n)}{\mathrm{i}(\alpha_n-\alpha)M_+(\alpha_n)}\frac{M_+(\alpha)}{(k_0+\alpha)} \tag{45}$$

$$\tilde{L}^{(1)}(\alpha)=\frac{K_n\mathrm{J}_1(K_na)(k_0+\alpha_n)}{\mathrm{i}(\alpha_n-\alpha)M_+(\alpha_n)}\frac{M_+(\alpha)}{(k_0+\alpha)} \tag{46}$$

while the second-order solutions become

$$\tilde{U}^{(2)}(\alpha)=\tilde{L}^{(2)}(\alpha)=\frac{M_+(\alpha)K_n\mathrm{J}_1(K_na)(k_0+\alpha_n)}{2\pi(k_0+\alpha)M_+(\alpha_n)}I_1(\alpha) \tag{47}$$

with

$$I_1(\alpha)=\int_{\mathcal{L}_-}\mathrm{e}^{\mathrm{i}\tau l}\frac{M_+^2(\tau)}{M(\tau)}\frac{(k_0-\tau)^2}{K_0^2(\tau)(\alpha_n-\tau)}\frac{d\tau}{(\tau+\alpha)}. \tag{48}$$

Due to the Jordan's lemma and the law of residues, the integration contour $\mathcal{L}_-$ can be deformed onto the branch-cuts C_1+C_2 and $C_1'+C_2'$ through the branch points $\tau=k_1$ and $\tau=k_0$, respectively. By substituting $\tau=k_0+it$, $\sqrt{\tau-k_0}=\sqrt{t}e^{i\pi 4}$ on C_1' and $\sqrt{\tau-k_0}=-\sqrt{t}e^{i\pi 4}$ on C_2' and using the properties

$$\mathrm{J}_n\left(\mathrm{e}^{\mathrm{i}\pi}z\right)=\mathrm{e}^{\mathrm{i}n\pi}\mathrm{J}_n(z)\ ,\quad \mathrm{H}_n^{(1)}\left(\mathrm{e}^{\mathrm{i}\pi}z\right)=-\mathrm{e}^{\mathrm{i}n\pi}\mathrm{H}_n^{(2)}(z)$$

gives

$$I_1(\alpha)=\frac{4\mathrm{i}M_+^2(k_0)(k_1-k_0)^4\mathrm{e}^{\mathrm{i}k_0l}\varepsilon_0\varepsilon_1\mathrm{J}_0^2\left(\sqrt{k_1^2-k_0^2}a\right)}{\pi a(\alpha_n+\alpha)}\left[\beta_1(a,l)-\beta_2(a,l,\alpha)\right] \tag{49}$$

where $\beta_1(a,l)$ and $\beta_2(a,l,\alpha)$ stand for

$$\beta_1(a,l)=\int_0^\infty\frac{t^2\mathrm{e}^{-tl}}{[t-\mathrm{i}(k_0-\alpha_n)]A(t)}dt \tag{50}$$

$$\beta_2(a,l,\alpha)=\int_0^\infty\frac{t^2\mathrm{e}^{-tl}}{[t-\mathrm{i}(k_0+\alpha)]A(t)}dt, \tag{51}$$

respectively with

$$\begin{aligned}A(t)=&\left[\varepsilon_1K_0^2K_1\mathrm{J}_1(K_1a)\mathrm{H}_0^{(1)}(K_0a)-\varepsilon_0K_1^2K_0\mathrm{J}_0(K_1a)\mathrm{H}_1^{(1)}(K_0a)\right]\\&\times\left[\varepsilon_0K_1^2K_0\mathrm{J}_0(K_1a)\mathrm{H}_1^{(2)}(K_0a)-\varepsilon_1K_0^2K_1\mathrm{J}_1(K_1a)\mathrm{H}_0^{(2)}(K_0a)\right].\end{aligned} \tag{52}$$

The integrals in (50) and (51) are to be evaluated numerically. Finally, the solution of the modified Wiener-Hopf equation (30) is determined as

$$P_1(a,\alpha)=\frac{K_n\mathrm{J}_1(K_na)(k_0+\alpha_n)}{\omega\varepsilon_1M_+(\alpha_n)}\left\{\frac{(k_0+\alpha)}{M_+(\alpha)(\alpha+\alpha_n)}-\frac{\mathrm{i}\mathrm{e}^{\mathrm{i}\alpha l}(k_0-\alpha)}{2\pi M_-(\alpha)}I_1(\alpha)\right\}. \tag{53}$$

3. **Analysis of the fields**

Considering the relation between H_ϕ and ψ and taking into account (31), the radiated magnetic field H_ϕ^{sc} in $\rho > a$ can be expressed as

$$H_\phi^{sc}(\rho, z) = \frac{\omega\varepsilon_0}{2\pi \mathrm{i}} \int_{\mathcal{L}} P_1(a, \alpha) \frac{\mathrm{H}_1^{(1)}(K_0\rho)}{K_0 \mathrm{H}_0^{(1)}(K_0 a)} \mathrm{e}^{-\mathrm{i}\alpha z} d\alpha \tag{54}$$

where the integration path $\mathcal{L}$ is lying in the strip $\Im m(-k_0) < \Im m(\alpha) < \Im m(k_0)$ as shown in Figure 2. Taking into account the asymptotic expression of the Hankel function $\mathrm{H}_1^{(1)}(K_0\rho)$ for large arguments and applying the saddle point technique, one obtains

$$H_\phi^{sc}(r, \theta) = D(\theta) \frac{\mathrm{e}^{\mathrm{i}k_0 r}}{k_0 r} \tag{55}$$

with

$$D(\theta) = -\frac{\omega\varepsilon_0}{\mathrm{i}\pi} \frac{P_1(a, k_0 \cos\theta)}{\sin\theta \mathrm{H}_0^{(1)}(k_0 a \sin\theta)}$$

and r and θ being defined as shown in Figure 3. On the other hand, the scattered magnetic

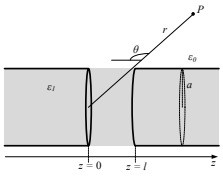

Fig. 3. Observation point P.

field H_ϕ in the region $\rho < a$ can be determined by the integral

$$H_\phi^{sc}(\rho, z) = \frac{\omega\varepsilon_1}{2\pi \mathrm{i}} \int_{\mathcal{L}} P_1(a, \alpha) \frac{\mathrm{J}_1(K_1\rho)}{K_1 \mathrm{J}_0(K_1 a)} \mathrm{e}^{-\mathrm{i}\alpha z} d\alpha. \tag{56}$$

In order to determine the reflected field, the above integral must be evaluated for $z < 0$. Taking into account the asymptotic behavior of $M_+(\alpha)$, (53) and the standard asymptotics related to the Bessel functions of the first and second type, one can show that the integrand in (56) tends to zero for $|\alpha| \to \infty$. This allows the application of the Jordan's lemma and by virtue of Jordan's lemma and the application of the law of residues, the above integral becomes equal to the sum of the residues related to the poles occurring at the simple zeros of $\mathrm{J}_0(K_1 a)$ lying in the upper half-plane, namely, at $\alpha = \alpha_m$'s. Defining the reflected field in this region as

$$H_\phi^{ref}(\rho, z) = \sum_{m=1}^{\infty} R_m \psi_m(\rho) e^{-i\alpha_m z} \tag{57}$$

one determines

$$R_m = \frac{\omega\varepsilon_1 P_1(a, \alpha_m)}{\alpha_m K_m a \mathrm{J}_1(K_m a)} \tag{58}$$

with

$$\psi_m(\rho) = K_m \mathrm{J}_1(K_m \rho). \tag{59}$$

Similarly, solving the integral (56) for $z > l$ in a similar fashion gives the transmitted magnetic field as

$$H_\phi^{tr}(\rho, z) = \sum_{m=1}^{\infty} T_m \psi_m(\rho) e^{i\alpha_m z} \tag{60}$$

with

$$T_m = -\frac{\omega\varepsilon_1 P_1\left(a, -\alpha_m\right)}{\alpha_m a K_m \mathrm{J}_1\left(K_1 a\right)}. \tag{61}$$

4. **Results**

The numerical analysis is made in order to investigate the effects of the parameters waveguide radius, gap width, frequency, relative permittivity of the filling material on the radiated magnetic field. The frequency range for the numerical analysis should be decided carefully, so that the dominant TM_{01} mode can propagate. Considering the first three zeros of $\mathrm{J}_0\left(z\right)$, one can find that the only propagating mode is TM_{01} for $2.4048 < ka < 5.5201$. The numerical analysis in this section is done within this frequency range. Also, in all the figures, the magnitude of the radiated field is normalized as described in [4]. In Figure 4, the results regarding different values of kl for $ka = 2.5$, $\varepsilon_r = 1$ is presented. It is understood from this figure that the analysis done in this paper has an excellent agreement with the one done by Elmoazzen and Shafai in 1974, when it is compared to Figure 3a in [4]. On the other hand, the dependence of the magnitude of the radiated field to ε_r, ka and kl is illustrated in Figures 5, 6 and 7, respectively. It is observed in Figure 6 that ka dependence is strong as the magnitude of the radiated field increases with increasing ka until the observation angle 140°. After that angle, it tends to vanish for higher values of ka. Also, one can see that for $ka = 6$, the magnitude of the radiated field drops significantly, as some of the energy is transferred to the TM_{02} mode, which starts propagating for $ka > 5.5201$. Besides, small ε_r dependence is observed in Figure 5, while negligibly small kl dependence is seen in Figure 7.

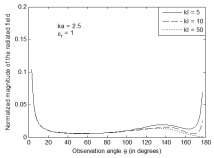

Fig. 4. The results for $\varepsilon_r = 1$.

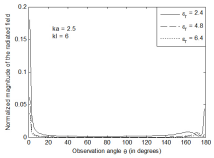

Fig. 5. ε_r dependence.

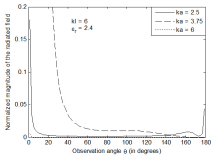

Fig. 6. ka dependence.

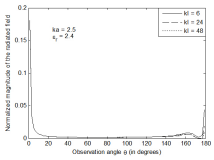

Fig. 7. kl dependence.

5. **Conclusions**

In this paper, TM wave scattering by a large circumferential gap on a circular waveguide filled with a dielectric material is investigated rigorously by applying direct Fourier transform and reducing the problem into the solution of a modified Wiener-Hopf equation of the first type. Classical Wiener-Hopf procedure is applied and the Wiener-Hopf equation is solved via a set of Fredholm integral equations of the second type. At the end the radiated field is investigated numerically and the dependence of its magnitude with respect to waveguide radius, relative permittivity, frequency and the gap width is illustrated graphically. Besides, it is found that the analysis done in this paper has an excellent agreement with the one in [4]. As this geometry is a good model for certain embedded antennas located inside organic tissues, the problem where the outer medium is complex, would be very interesting to analyze for future studies, and thus, develop a more accurate model for such applications.

6. **Appendix**

Convergence of $\beta_1(a,l)$ and $\beta_2(a,l,\alpha)$

In order to show the convergence of the integrals, we primarily split them into sums of two terms:

$$\beta_1(a,l) = \int_0^1 \frac{t^2 \mathrm{e}^{-tl}}{[t - \mathrm{i}(k_0 - \alpha_n)]\, A(t)} dt + \int_1^\infty \frac{t^2 \mathrm{e}^{-tl}}{[t - \mathrm{i}(k_0 - \alpha_n)]\, A(t)} dt \tag{A.1}$$

$$\beta_2(a,l;\alpha) = \int_0^1 \frac{t^2 \mathrm{e}^{-tl}}{[t - \mathrm{i}(k_0 + \alpha)]\, A(t)} dt + \int_1^\infty \frac{t^2 \mathrm{e}^{-tl}}{[t - \mathrm{i}(k_0 + \alpha)]\, A(t)} dt \tag{A.2}$$

Since the integrands are continuous for $t \in [0,1]$ in the above integrals, we can easily say that the first integrals are convergent. For the second integrals, by utilizing the following asymptotic expansion for $t \to \infty$,

$$A(t) \simeq -\frac{2t^2}{\pi a}\left\{\varepsilon_1^2 \cos^2(ta - 3\pi/4) + \varepsilon_0^2 \cos^2(ta - \pi/4)\right\}, \tag{A.3}$$

it is possible to use limit comparison test with

$$g(t) = \frac{\pi a e^{-tl}}{2t\left\{\varepsilon_1^2 \cos^2(ta - 3\pi/4) + \varepsilon_0^2 \cos^2(ta - \pi/4)\right\}}, \tag{A.4}$$

which is continuous except at $t = 0$. For $t > 1$

$$\left|\frac{\pi a e^{-tl}}{2t\left\{\varepsilon_1^2 \cos^2(ta - 3\pi/4) + \varepsilon_0^2 \cos^2(ta - \pi/4)\right\}}\right| \leq \frac{\pi a e^{-tl}}{2t\varepsilon_0^2}. \tag{A.5}$$

holds. Since

$$\int_1^\infty \frac{\pi a e^{-tl}}{2t\varepsilon_0^2} dt \tag{A.6}$$

converges,

$$\int_1^\infty \frac{\pi a e^{-tl}}{2t\left\{\varepsilon_1^2\cos^2(ta-3\pi/4)+\varepsilon_0^2\cos^2(ta-\pi/4)\right\}}dt \tag{A.7}$$

is absolutely convergent. Moreover,

$$\lim_{t\to\infty}\left|\frac{\frac{t^2\mathrm{e}^{-tl}}{[t-\mathrm{i}(k_0-\alpha_n)]A(t)}}{\frac{\pi a e^{-tl}}{2t\left\{\varepsilon_1^2\cos^2(ta-3\pi/4)+\varepsilon_0^2\cos^2(ta-\pi/4)\right\}}}\right|=1 \tag{A.8}$$

$$\lim_{t\to\infty}\left|\frac{\frac{t^2\mathrm{e}^{-tl}}{[t-\mathrm{i}(k_0+\alpha)]A(t)}}{\frac{\pi a e^{-tl}}{2t\left\{\varepsilon_1^2\cos^2(ta-3\pi/4)+\varepsilon_0^2\cos^2(ta-\pi/4)\right\}}}\right|=1. \tag{A.9}$$

Since

$$\int_1^\infty \frac{\pi a e^{-tl}}{2t\left\{\varepsilon_1^2\cos^2(ta-3\pi/4)+\varepsilon_0^2\cos^2(ta-\pi/4)\right\}}dt \tag{A.10}$$

is absolutely convergent, we conclude that second integrals in (A.1) and (A.2) are also convergent. Therefore, the improper integrals (50) and (51) are convergent.

REFERENCES

[1] *G. Cinar and A. Buyukaksoy*, Diffraction by a thick impedance half-plane with a different end face impedance, Electromagnetics, **22**(2002), No. 7, 565-580.

[2] *G. Cinar*, Wiener-Hopf analysis of plane wave diffraction by an impedance strip attached on a perfectly conducting half-plane, Electromagnetics, **29**(2009), No. 2, 165-184.

[3] *T. M. Dunster*, Electromagnetic wave scattering by two parallel infinite dielectric cylinders, Studies Appl. Math., **131**(2013), No. 3, 302-316.

[4] *Y. E. Elmoazzen and L. Shafai*, Mutual coupling between two circular waveguides, IEEE Trans. Antennas Propagat., **22**(1974), No. 6, 751-760.

[5] *J. B. Lawrie*, Axisymmetric radiation from a finite gap in an infinite, rigid, circular duct, IMA J. Appl. Math., **40**(1988), No. 2, 113-128.

[6] *R. Mittra and S. W. Lee*, Analytical techniques in the theory of guided waves, New York: McMillan, 1971.

[7] *N Morita and Y. Nakanishi*, Circumferential gap in a TE_{01}-mode transmitting multimode circular waveguide, IEEE Trans. Microw. Theory Tech., **16**(1968), No. 3, 183-189.

[8] *H. Ozturk, G. Cinar and O. Y. Cinar*, TEM wave radiation from a dielectric-filled coaxial waveguide with a large circumferential gap on its outer wall, J. Appl. Math. Phys., **66**(2015), No. 4, 1299-1313.

[9] *H. Ozturk and G. Cinar*, Scattering of a TEM wave by a large circumferential gap on a coaxial waveguide, J. Electromagn. Waves Appl., **27**(2013), No. 5, 615-628.

[10] *J. K. Park and H. J. Eom*, TM scattering by a gap on a circular waveguide, Microw. Opt. Tech. Lett., **37**(2013), No. 2, 146-148.

[11] *B. Polat*, Diffraction of acoustic waves by a cylindrical impedance rod of finite length, Z. Angew. Math. Mech., **79**(1999), No. 8, 555-567.

[12] *S. S. Sautbekov*, Diffraction of plane wave by strip with arbitrary orientation of wave vector, Prog. Electromagn. Res. M., **21**(2011), 117-131.

[13] *S. Seran, J. P. Donohoe and E. Topsakal*, Diffraction from a material loaded tandem slit, IEEE Trans. Antennas Propagat., **57**(2009), No. 11, 3500-3511.

[14] *L. S. Sheingold and J. E. Storer*, Circumferential gap in a circular wave guide excited by a dominant circular-electric wave, J. Appl. Phys., **25**(1954), No. 5, 545-552.

[15] *I. H. Tayyar, A. Buyukaksoy and A. Isikyer*, Wiener-Hopf analysis of the parallel plate waveguide with finite length impedance loading, Radio Sci., (2008), 43:doi:10.1029/2007RS003768.